

NASA
TP
1780
c.1

NASA Technical Paper 1780

LOAN COPY
AFWL TECHNICAL
KIRTLAND AIR



Cold-Air Investigation of First Stage of $4\frac{1}{2}$ -Stage, Fan-Drive Turbine With Average Stage-Loading Factor of 4.66

Warren J. Whitney, Thomas P. Moffitt,
and Frank P. Behning

JANUARY 1981

NASA



NASA Technical Paper 1780

Cold-Air Investigation of First Stage
of $4\frac{1}{2}$ -Stage, Fan-Drive Turbine With
Average Stage-Loading Factor of 4.66

Warren J. Whitney, Thomas P. Moffitt,
and Frank P. Behning
*Lewis Research Center
Cleveland, Ohio*

NASA

National Aeronautics
and Space Administration

**Scientific and Technical
Information Branch**

1981

Summary

The design procedure and the development of the blading geometry for the 4½-stage turbine are discussed. The experimental results obtained with the first stage, operated as a single-stage turbine, are presented.

The design procedure showed that a free-vortex design could meet the requirements without incurring any serious problems such as excessive turning, negative reaction, or high Mach number. The results of the cold-air tests of the single-stage turbine showed that the turbine developed design work (stage loading factor of 5.26) at an efficiency of 0.86, which was the efficiency predicted by a reference method. The mass flow at this condition was 1.024 of the design value. The highest efficiency obtained over the range of test conditions was 0.88, which occurred at design speed and a pressure ratio of 1.407, corresponding to a stage-loading factor of 4.35. The efficiency at this condition was 0.003 higher than predicted by the reference method.

Introduction

In recent years the NASA Lewis Research Center has devoted a part of its turbine research effort to the investigation of turbines with high stage-loading factors (refs. 1 to 4, e.g.). Turbines with high stage-loading factors (i.e., the ratio of change in tangential velocity to blade speed) result when a direct-drive fan turbine is desired and the turbine speed is limited by the fan tip speed, especially for high-bypass-ratio engines. This type of turbine is generally characterized by shrouded rotor blades, large turning angles in both rotor and stator blade rows, and nearly symmetrical mean-radius velocity diagrams.

One of the projects in this program was a cost-sharing undertaking between Lewis Research Center and Pratt & Whitney Aircraft (P&WA) of East Hartford, Connecticut, to investigate a 4½-stage, fan-drive turbine with an average stage-loading factor of 4.66. The turbine design evolved from a study made by P&WA of the engine requirements for an advanced transport airplane. The turbine aerodynamic and mechanical designs were conducted by the contractor. The pertinent features of the aerodynamic design, which the contractor discusses

in reference 5 were (1) forced vortex flow with tailored radial work distribution and (2) controlled position of the boundary-layer transition point on the airfoil suction surface to achieve a minimized profile loss. The contractor had anticipated an efficiency of 0.886 for the 4½-stage turbine.

A one-half-scale, cold-air model of the turbine was then fabricated by P&WA, and the turbine performance was obtained in cold-air tests at the Lewis Research Center. The results of these tests are described in references 6 and 7. In reference 6 the 4½-stage turbine developed design work at an efficiency of 0.855, which was 0.031 lower than the value anticipated by the contractor. The efficiency estimate for this turbine based on NASA prediction methods and experience (refs. 8 and 9) was 0.862. The stage group tests of reference 7 verified the overall performance obtained in reference 6 and showed that all the stages operated reasonably close to their expected performance level.

At the time the contract was placed with P&WA, a companion in-house project was begun to develop a turbine with the same performance requirements. It was planned to design, fabricate, and test the complete in-house, 4½-stage, work-factor-of-4.66 turbine. The design of the in-house turbine employed more conventional assumptions such as free-vortex flow and constant radial work extraction, as were used in reference 1.

After the design of the NASA 4½-stage turbine was completed, including the development of all the blading geometry, the program was curtailed, and all subsequent research was limited to the first stage. The first stage was fabricated, and its performance was determined in cold air. This report describes the design of the 4½-stage turbine and presents the performance results obtained with the first stage. The performance results are compared with those of the P&WA first stage from reference 7. The cold-air performance was obtained with inlet conditions of total temperature and total pressure maintained at 378 K (680° R) and 2.4 atmospheres, respectively. The turbine was operated at 80, 90, 100, and 110 percent of design speed, and total-pressure ratio was varied over a range (bracketing design pressure ratio) at each speed.

Symbols

A area, m²; ft²

- D_m mean diameter, constant for all four stages, m; ft
- g force-mass conversion constant, 1; 32.174 ft/sec²
- h specific enthalpy, J/g; Btu/lb
- N rotative speed, rpm
- n number of stages
- P absolute pressure, N/m²; lb/ft²
- R gas constant for mixture of air and combustion products used in this investigation, 288 J/(kg)(K): 53.527 (ft-lb)/(lb)(°R)
- T temperature, K; °R
- U blade velocity, m/sec; ft/sec
- U_m effective mean blade speed, $(\pi D_m N)/60$, m/sec; ft/sec
- V absolute gas velocity, m/sec; ft/sec
- W gas velocity relative to moving blade, m/sec; ft/sec
- w mass flow rate (sum of air and fuel flow rates), kg/sec; lb/sec
- α absolute gas flow angle measured from axial direction, deg
- $\bar{\alpha}$ average absolute gas flow angle at turbine outlet measured from axial direction irrespective of sign, used in eq. (2), deg
- β angle of gas flow relative to moving blade measured from axial direction, deg
- γ ratio of specific heats, 1.398 for mixture of air and combustion products used in this investigation
- δ ratio of inlet pressure to U.S. standard sea-level pressure
- ϵ function of γ , $(0.73959/\gamma)[(\gamma+1)/2]^{\gamma/(\gamma-1)}$
- η efficiency based on total-pressure ratio
- θ_{cr} squared ratio of critical velocity at turbine inlet to critical velocity of U.S. standard sea-level air
- τ torque, N-m; ft-lb
- Subscripts:
- cr condition at Mach 1
- m mean radius
- u tangential component
- 0 station at turbine inlet (fig. 6)
- 1 station at stator outlet on velocity diagram
- 2 station at rotor outlet on velocity diagram
- I station at stator inlet (fig. 6)
- II station at turbine outlet (fig. 6)
- Superscript:
- ' total state

Turbine Design

The 4½-stage in-house turbine was of the free-vortex type with simplified or conventional design features.

Design Requirements

The requirements of the 4½-stage in-house turbine were as follows:

Number of stages, n	4
Average stage-loading factor, $\Delta h \times 10^3/nU_m^2$	4.66
Equivalent specific work, $\Delta h/\theta_{cr}$, J/g;	
Btu/lb	102.58; 44.1
Equivalent mass flow, $\epsilon w\sqrt{\theta_{cr}/\delta}$, kg/sec;	
lb/sec	5.84; 12.875
Equivalent mean blade speed, U_m , m/sec;	
ft/sec	74.179; 243.37
Mean diameter, D_m , m; ft	0.4572; 1.5
Equivalent rotative speed, $N/\sqrt{\theta_{cr}}$, rpm	3098.7

It can be seen that these requirements differ slightly from those of reference 5. Notably the specific work is 0.98 that of the P&WA turbine and the mass flow density, $(\epsilon w\sqrt{\theta_{cr}/\delta})/D_m^2$, is 1.06 that of the P&WA turbine.

These requirements were those proposed for the contract turbine early in the negotiation period. The requirements were then frozen for the in-house turbine program; some small changes in the requirements were subsequently incorporated in the design of the contract turbine. These differences are small, however, and should not effect any changes in performance expectations between the two turbines.

Stage Work Split

The work splits considered for this application are tabulated as follows, as fractions of the total work done by the individual stages:

Stage	Work split			
	A	B	C	D
1	0.25	0.2923	0.3223	0.2819
2		.2621	.2522	.2725
3		.2349	.2248	.2449
4		.2106	.2006	.2006
Efficiency ratio	1.0000	1.0010	1.0020	1.0004

Work split A is equal actual work per stage, and work split B is equal equivalent work per stage. Work split C was obtained by increasing the first-stage work of split B by 10 percent and decreasing the

second, third, and fourth stages of split B by 4 to 5 percent. The work split used was split D, which is equal equivalent work per stage modified to increase the work in stages 2 and 3 and reduce the work in stages 1 and 4. These modifications were made from the considerations of (1) limiting the first-stage stator angle to about 65° , (2) maintaining subsonic relative velocities throughout the turbine, and (3) reducing the turning angle and diffusion requirement of the outlet turning vanes. The overall four-stage turbine efficiency, normalized by that of split A, is included in the table as the efficiency ratio. The efficiencies of the different work splits were so close that efficiency did not influence the selection.

Velocity Diagrams

A free-vortex type of velocity diagram was developed for the $4\frac{1}{2}$ -stage turbine to meet the required total work and the selected stage work split, D. The mean radius diagram was made symmetrical with respect to tangential velocity components; that is, $V_{u,1,m} = W_{u,2,m}$ and $W_{u,1,m} = V_{u,2,m}$. The ratio of axial velocity to blade speed was maintained in the optimum region, as indicated by figure 3.37 of reference 10. The axial velocity was increased by 2 to 6 percent across the rotor blade rows and decreased by like amounts in the stator blade rows. This axial velocity variation increased the reaction in the rotor blade rows and decreased the reaction across the stators.

The resulting velocity diagram is shown in figure 1, where no obviously detrimental features such as low or negative reaction, excessive turning, or high Mach number can be seen. All the blading sections operate with some positive reaction. The maximum turning occurred at the first-stage rotor hub section, 120.6° . The maximum critical velocity ratio was 0.999 and occurred at the third-stage rotor blade hub section. The turning requirement of the outlet turning vanes is about the same as in references 1 and 3. The velocity diagram of the P&WA $4\frac{1}{2}$ -stage turbine (ref. 6) is shown in figure 2 for comparison.

Blade Design

The flowpath for the $4\frac{1}{2}$ -stage in-house turbine is shown in figure 3. An axial chord of 2.8 centimeters (1.1 in.) was selected for the rotor blading. The average axial chord for the stators of the second, third, and fourth stages was also 2.8 centimeters, the first stage being 2.3 centimeters (0.9 in.). This value, 2.8 centimeters (1.1 in.) resulted in reasonable aspect ratios for the downstream stages. For stages 1 and 2, smaller chord blading might be preferred; however,

this would have increased the problem of manufacturing tolerances.

The number of blades was determined by using Zweifel loading coefficients (refs. 11 and 12) of 0.85 for the stator blade rows and 0.95 for the rotor blade rows. The blade channels were laid out at constant radii at the hub, mean, and tip sections at the blade outlet station. The quasi-three-dimensional method used is the same as that described in reference 1. All blade rows except for the first-stage stator and the outlet turning vanes were laid out to provide a divergent-convergent area distribution such that the maximum passage orthogonal occurred at about the midchord position. This resulted in thin blades in which the diffusion occurred on the front portion of the pressure surface with almost no diffusion on the suction surface. The pertinent blading design features are listed in table I for the $4\frac{1}{2}$ -stage turbine. As mentioned in the introduction, the fabrication and testing were limited to the first stage. The first stage surface velocity distributions are shown in figure 4 and the blading coordinates are given in table II. The first-stage blading passages and profiles are shown in figure 5. The flowpath and instrumentation stations of the single-stage turbine are shown in figure 6.

Apparatus, Instrumentation, and Procedure

The test facility is that described in reference 6. The turbine airflow was measured with a venturi meter. The fuel flow (natural gas) was metered with a flat-plate orifice. Both of these flow-rate measurements required an upstream pressure measurement, an upstream temperature measurement, and a measurement of differential pressure across the flowmeter element. The turbine mass flow was obtained as the sum of the fuel and air flows.

The turbine shaft speed was measured with a magnetic pickup and a square tooth sprocket that was mounted on the turbine shaft. An electronic counter was used to convert the electrical impulses to shaft rotative speed. Turbine torque was measured as the reaction torque on the dynamometer stator with a strain-gage load cell. The dynamometer stator was cradled and supported by a high-pressure oil film (hydrostatic trunnion bearing).

The turbine test section was instrumented as shown in figure 6. The turbine inlet total temperature T_1' was determined from 10 temperature measurements at station 0—two rakes of five each. These temperatures were corrected for recovery coefficient and then averaged to obtain the inlet total temperature T_1' . The static pressure P_1 was obtained

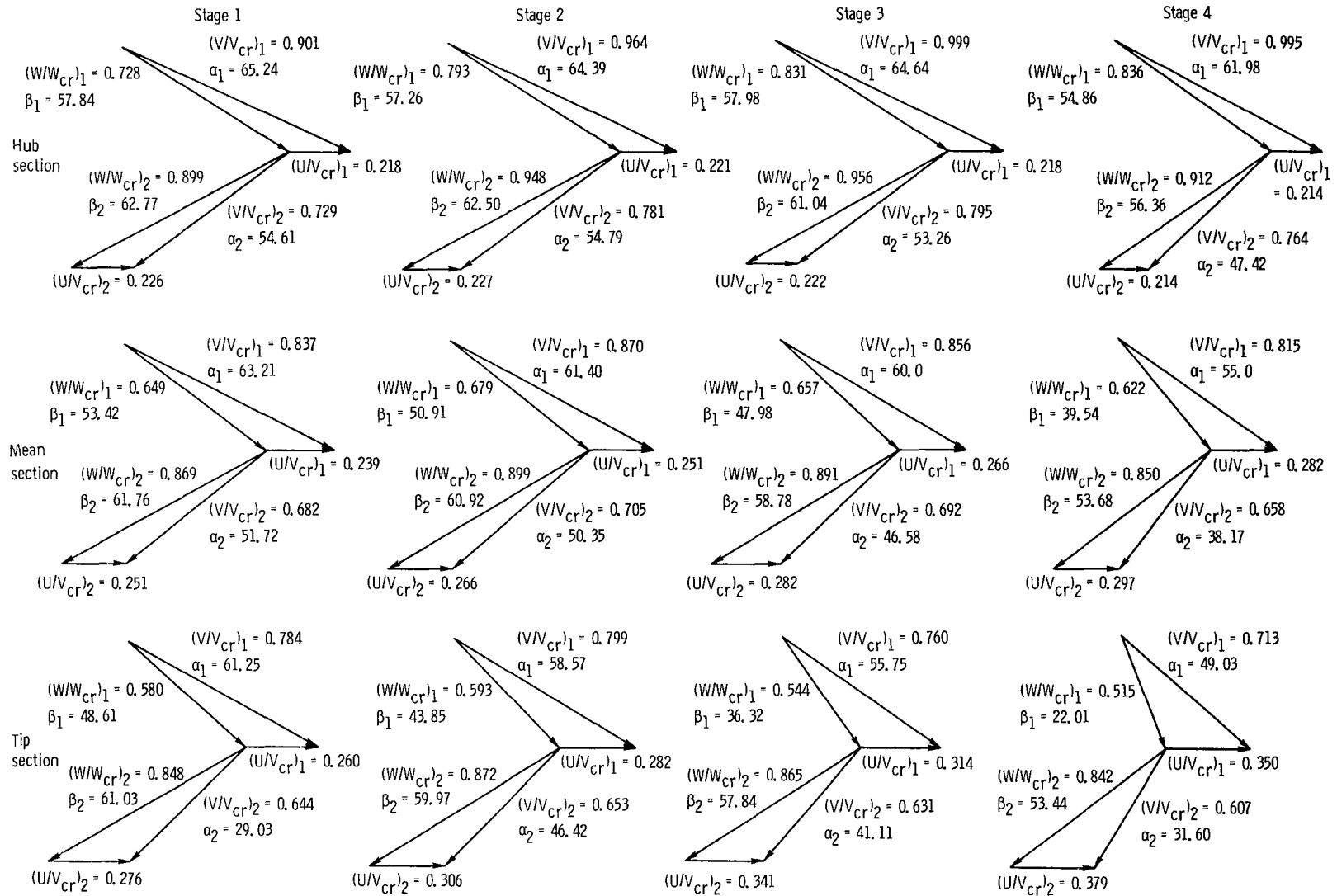


Figure 1. - Velocity diagram of $4\frac{1}{2}$ -stage, in-house turbine with work factor of 4.66.

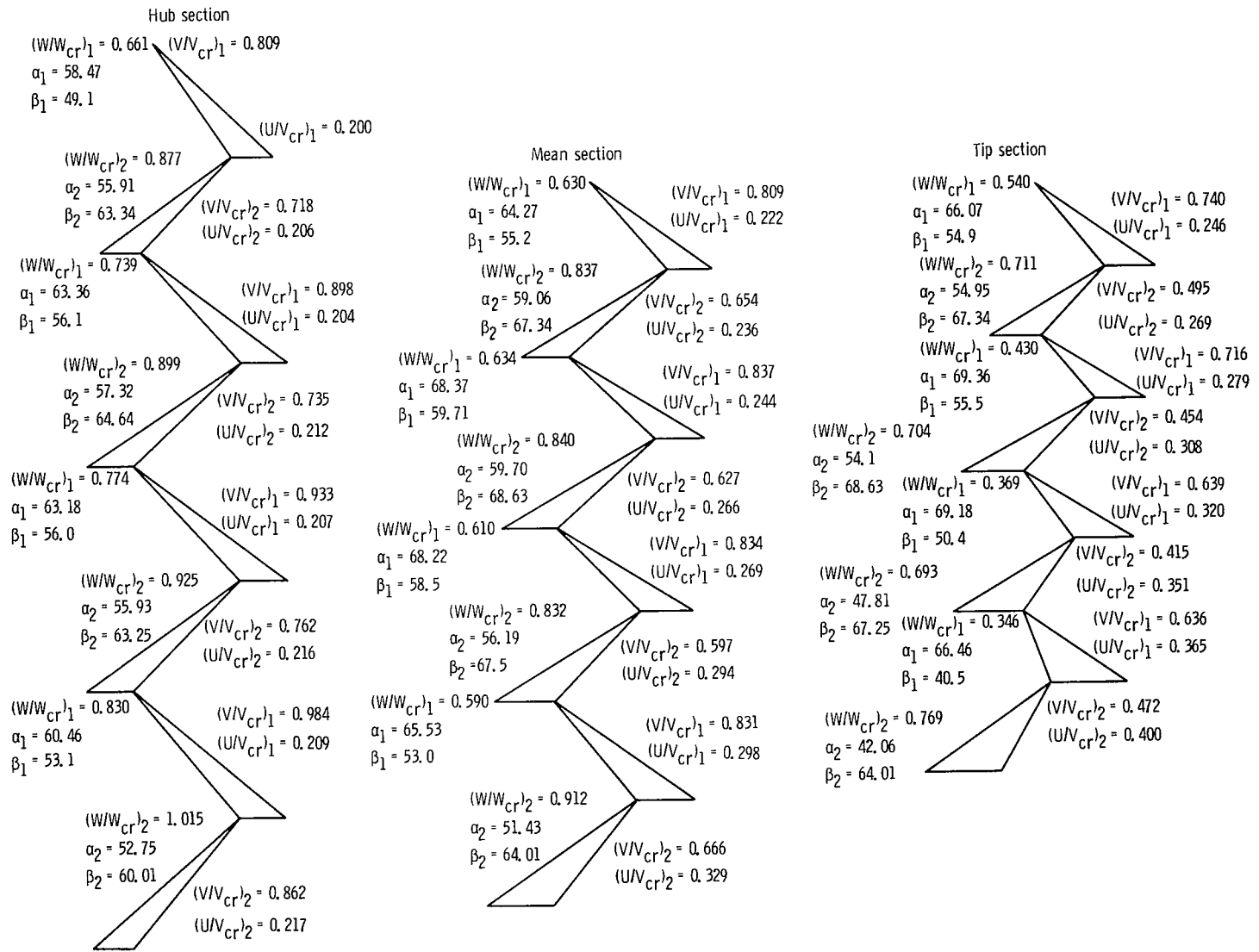


Figure 2. - Velocity diagram of $4\frac{1}{2}$ -stage, contractor-designed turbine with work factor of 4.66.

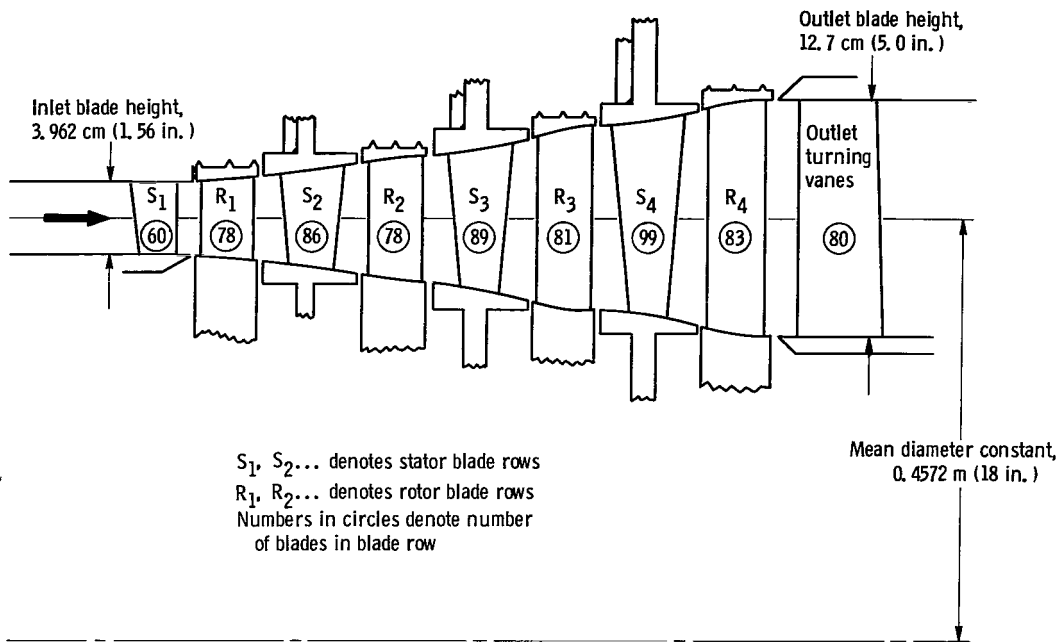


Figure 3. - Flowpath through $4\frac{1}{2}$ -stage in-house turbine.

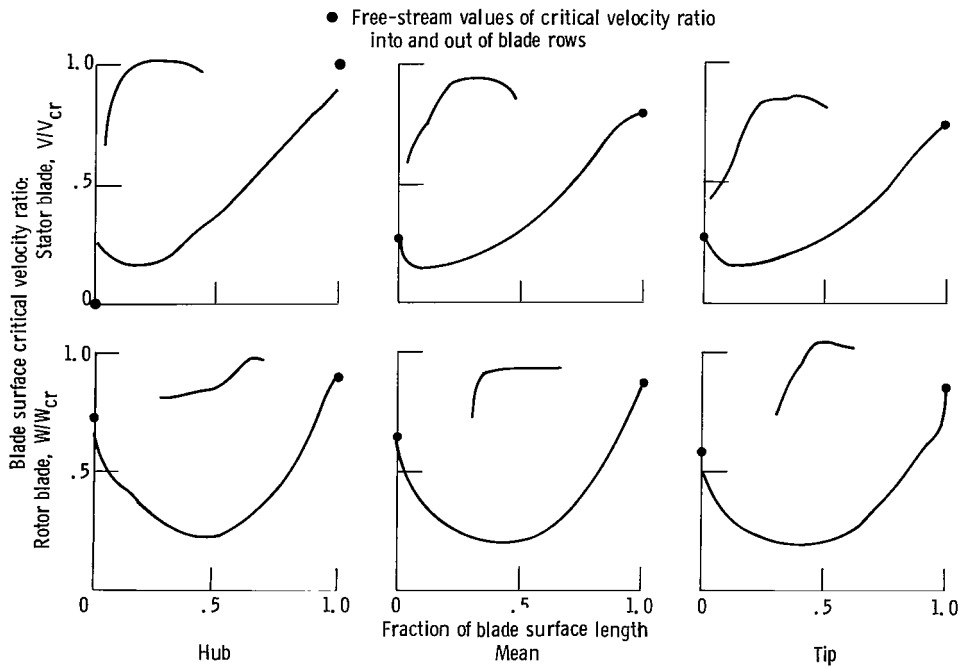


Figure 4. - Design blade surface velocity distributions.

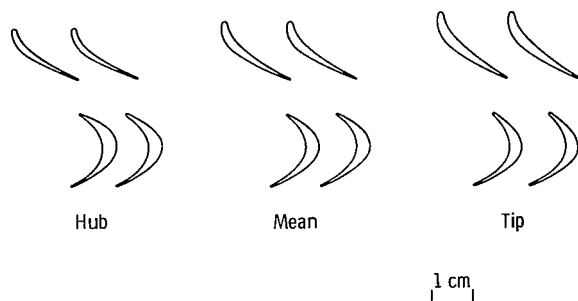
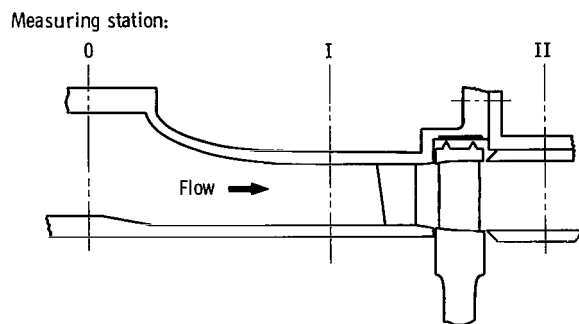
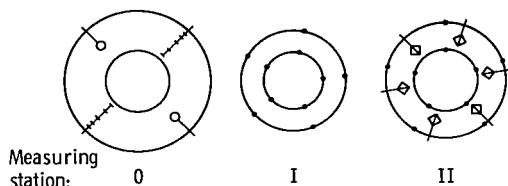


Figure 5. - Turbine blading passages and profiles.



(a) Test section.

- Wall static-pressure tap
- +—+— Thermocouple rake
- Kiel total-pressure probe
- ◇— Combination angle and total-pressure probe



(b) Instrumentation (looking upstream).

Figure 6. - Test section and instrumentation location.

by averaging the readings from the 10 static wall taps at the turbine inlet (station I). The total pressure was then calculated from the following equation:

$$\frac{P'_I}{P_I} = \left[\frac{1}{2} + \sqrt{\frac{1}{4} + \left(\frac{\gamma-1}{2g\gamma} \right) \left(\frac{w}{P_I A_I} \right)^2 RT'_I} \right]^{\frac{\gamma}{\gamma-1}} \quad (1)$$

as in reference 6.

At the turbine outlet (station II) the static pressure was also obtained by averaging the readings from 10 static wall taps. Turbine exit flow angle was

measured by six self-aligning combination probes. For each data point each probe was stepped radially to the centers of five equal annular areas. The exit angle α_{II} was then determined by averaging the absolute value of the 30 readings. The total temperature was determined from the inlet total temperature and the specific enthalpy drop, which in turn was determined from the torque, speed, and mass flow measurements. The equation for outlet total pressure is

$$\frac{P'_{II}}{P_{II}} = \left[\frac{1}{2} + \sqrt{\frac{1}{4} + \left(\frac{\gamma-1}{2\gamma} \right) \left(\frac{w}{P_{II} A_{II}} \right)^2 \frac{RT'_{II}}{\cos^2 \alpha_{II}}} \right]^{\frac{\gamma}{\gamma-1}} \quad (2)$$

Data were obtained at 80, 90, 100, and 110 percent of design speed over a range of pressure ratio bracketing design specific work output. Inlet conditions of temperature and pressure were maintained at 378 K (680° R) and 2.4 atmospheres, respectively.

Results and Discussion

This section discusses the experimental results obtained with the single-stage, free-vortex turbine. These results are then compared with the results of the single-stage configuration of reference 7.

Performance of Single-Stage, Free-Vortex Turbine

The equivalent torque τ_c/δ is shown as a function of the total-pressure ratio P'_I/P'_{II} for the four speeds in figure 7 (a). The data correlate well at all speeds. The greatest deviation from the smooth curves was about 1/2 to 1 percent. The torque curves also indicate that the turbine was not near limiting loading for the range of conditions covered.

The equivalent mass flow $\epsilon w \sqrt{\theta_{cr}}/\delta$ is shown as a function of the total-pressure ratio P'_I/P'_{II} in figure 7(b). The data correlate closely with the smooth curves. The maximum scatter was about 0.2 percent. The 100-percent-design-speed data, which cover the greatest range of pressure ratio, indicated close to choking conditions at a pressure ratio of 1.75. Design equivalent mass flow was 5.84 kilograms per second (12.875 lb/sec).

The equivalent specific work output $\Delta h/\theta_{cr}$ is shown in figure 7(c) as a function of the pressure ratio P'_I/P'_{II} for the four equivalent speeds. At equivalent design speed the turbine developed the design equivalent work output, 28.93 joules per gram (12.436 Btu/lb), at a pressure ratio of 1.54. The

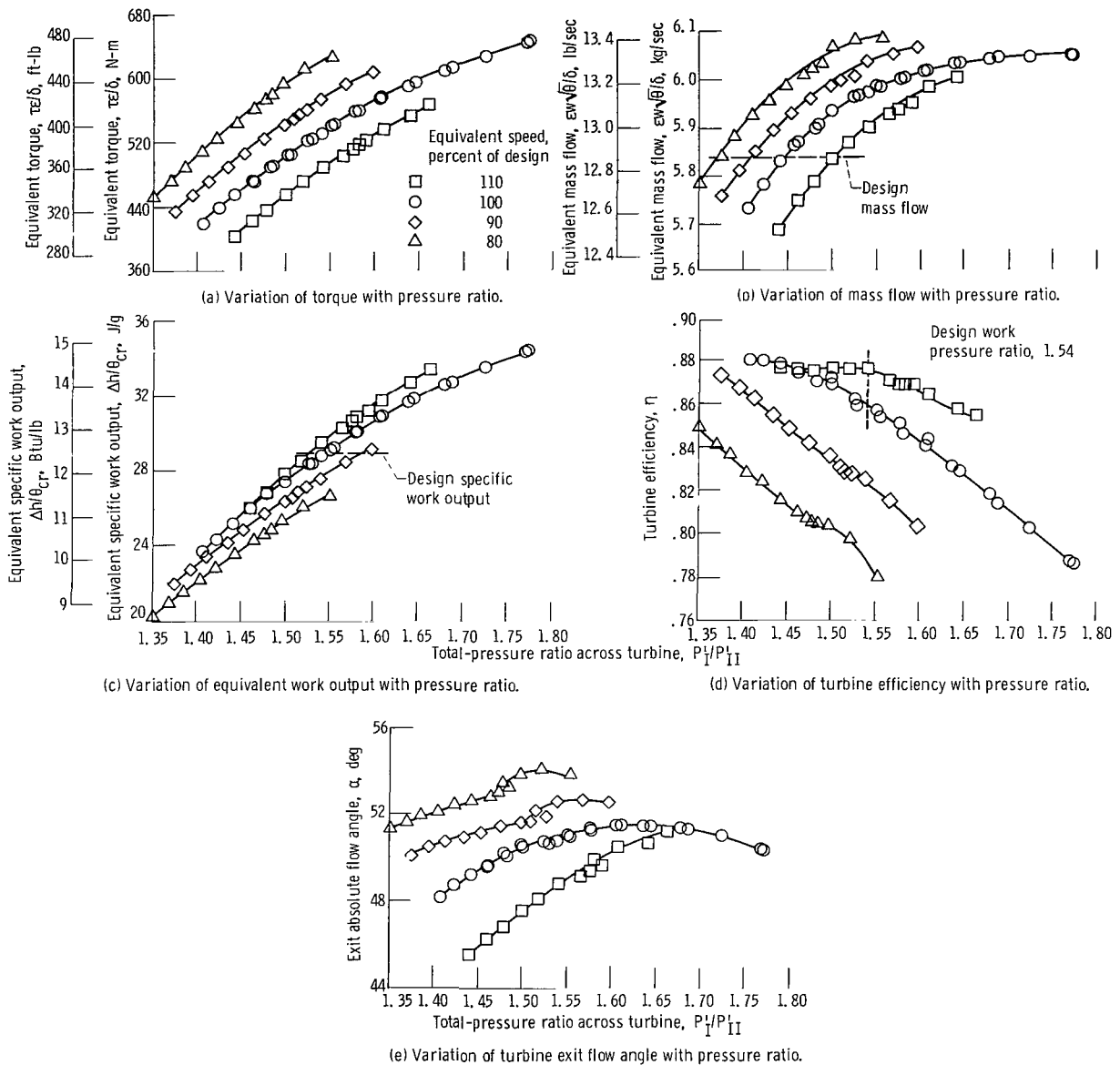


Figure 7. - Experimental results obtained with single-staged, free-vortex turbine.

efficiency corresponding to this pressure ratio and specific work output was 0.86.

The efficiency trends are shown in figure 7(d) as a function of the total-pressure ratio P_1/P_{11} . The efficiency at design work pressure ratio, 1.54, at design speed was 0.86. The mass flow at this condition (fig. 7(b)) was 5.978 kilograms per second (13.18 lb/sec), or 1.024 of the design mass flow. The highest efficiency was 0.88 and occurred at design speed at a pressure ratio of 1.407 (fig. 7(d)). The stage work factor at this condition was 4.35.

The exit flow angle is shown in figure 7(e) for the range of test conditions. The exit flow angle at the design work output pressure ratio, 1.54, at design speed was 51° . The average exit angle from the design velocity diagram is 51.77° .

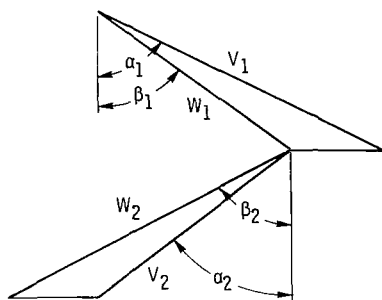
Velocity Diagram

The velocity diagram was calculated from the experimental results for the condition of design specific work output and design speed. In this

procedure it was assumed that the entire flow field could be represented by a single diagram at the mean radius. The derived diagram was constructed by using the experimentally measured values of mass flow, specific work output, rotative speed, efficiency, and exit flow angle. The experimentally derived diagram is compared with the design diagram in figure 8. The flow out of the stator appears to be underturned by about $\frac{1}{3}^\circ$, and the flow out of the rotor blade appears to be underturned by about 1° . The excess mass flow (1.024 of the design value) indicates that both the stator blade and rotor blade outlet angles should be closed by 0.7° .

Efficiency—Stage-Loading Factor Trends

The design-speed data, with efficiency as a function of stage-loading factor, are shown in figure 9. Included in the figure are the design-speed data from the single-stage turbine of reference 7. At its design work output, corresponding to a stage-loading factor of 5.26, the subject turbine operated at an efficiency of 0.86, which was the value predicted by



	Design value		Experimentally derived value	
	m/sec	ft/sec	m/sec	ft/sec
Velocity				
$V_{u,1}$	232.0	761.3	236.4	775.6
$V_{u,2}$	157.8	517.9	153.7	504.3
$V_{x,1}$	117.2	384.4	121.2	397.6
$V_{x,2}$	124.6	408.8	125.4	411.5
V_1	259.9	852.8	265.7	871.6
V_2	201.1	659.8	198.4	650.9
W_1	196.6	645.0	202.8	665.2
W_2	263.4	864.1	259.8	852.5
Angle, deg				
α_1	63.21		62.86	
β_1	53.42		53.28	
α_2	51.72		50.78	
β_2	61.76		61.14	

Figure 8. - Comparison of equivalent design velocity diagram at mean radius with that calculated from experimental results.

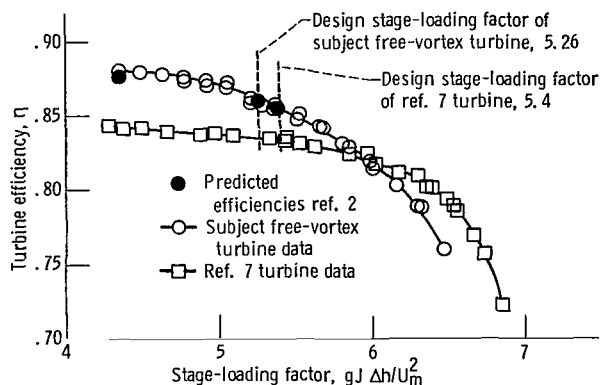


Figure 9. - Efficiency comparison of two turbines at design speed as a function of stage-loading factor.

reference 2. At a stage-loading factor of 5.4, which was the design value for the reference 7 turbine, the subject turbine efficiency (0.855) was very close to the predicted value (0.856). The efficiency of the reference 7 turbine at this stage-loading factor was (0.835), as mentioned in reference 7. The highest efficiency (0.88) of the subject turbine, which occurred at a stage-loading factor of 4.35 (pressure ratio, 1.407), was 0.003 higher than the predicted value.

Exit Flow Angle Variation

The experimental and design radial variations in turbine exit angle are shown in figure 10 for both the subject turbine and the reference turbine. In figure 10(a) the exit angle of the subject turbine follows the design trend closely, the maximum deviation being about 3° . The design trend is not this closely duplicated by the reference 7 turbine (fig. 7(b)). The exit angle is 4° to 6° greater than design over the lower 60 percent of the blade span. This deviation would cause an incidence angle of this magnitude in the second-stage stator of the reference turbine. This may have been a contributing factor that caused the second stage to have the lowest stage efficiency of the four stages in reference 7.

Summary of Results

A $4\frac{1}{2}$ -stage turbine with an average stage-loading factor of 4.66 was designed to meet the requirements of driving the fan of a turbofan engine for an advanced transport airplane. The geometry was developed for the complete turbine. The first stage of this turbine was fabricated, and its performance was determined in cold air. The following pertinent results were obtained from the design procedure and the experimental investigation:

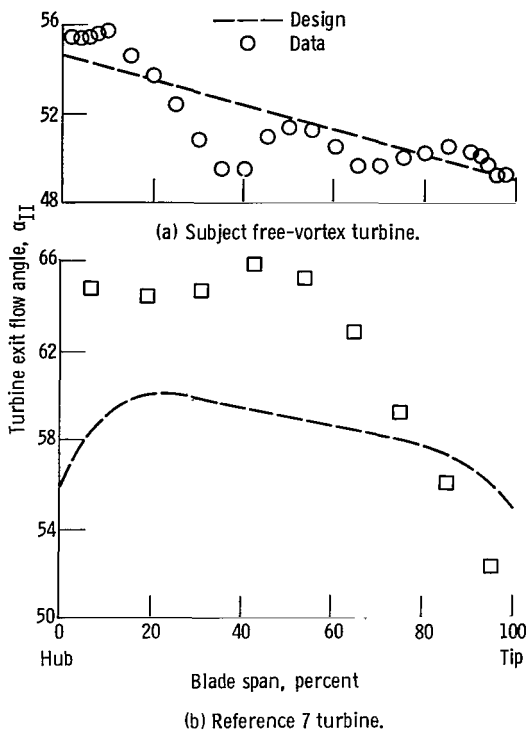


Figure 10. - Radial variation in exit flow angle for two turbines at design speed and design specific work output.

1. The design study and layout of the 4½-stage turbine showed that a free-vortex design could meet the design requirements with no obviously severe problems such as excessive turning, negative reaction, or high Mach number.

2. The first stage of the turbine, operated as a single stage, developed design work (stage-loading factor of 5.26) at an efficiency of 0.86, which was the efficiency predicted by a reference method. The mass flow at this condition was 1.024 of the design value.

3. The highest efficiency obtained was 0.88, which occurred at design speed at a pressure ratio of 1.407, corresponding to a stage-loading factor of 4.35. The efficiency at this condition was 0.003 higher than the predicted value.

Lewis Research Center,
National Aeronautics and Space Administration,
Cleveland, Ohio, June 10, 1980,
505-32.

References

1. Whitney, Warren J.; Schum, Harold J.; and Behning, Frank P.: Cold-Air Investigation of a 3½-Stage Fan-Drive Turbine with a Stage Loading Factor of 4 Designed for an Integral Lift Engine. I—Turbine Design and Performance of First Stage. NASA TM X-3289, 1975.
2. Whitney, Warren J.; Schum, Harold J.; and Behning, Frank P.: Cold-Air Investigation of a 3½-Stage Fan-Drive Turbine with a Stage Loading Factor of 4 Designed for an Integral Lift Engine. II—Performance of 2-Stage, 3-Stage, and 3½-Stage Configurations. NASA TM X-3482, 1977.
3. Walker, N. D.; and Thomas, M. W.: Experimental Investigation of a 4½-Stage Turbine with Very High Stage Loading Factor. II—Turbine Performance. NASA CR-2363, 1974.
4. Wolfmeyer, G. W.; and Thomas, M. W.: Highly Loaded Multi-Stage Fan Drive Turbine—Performance of Initial Seven Configurations. NASA CR-2362, 1974.
5. Webster, P. F.: Design of a 4½-Stage Turbine with a Stage Loading Factor of 4.66 and High Specific Work Output. NASA CR-2659, 1976.
6. Whitney, Warren J.; et al.: Cold-Air Investigation of a 4½-Stage Turbine with Stage Loading Factor of 4.66 and High Specific Work Output. I—Overall Performance. NASA TM X-3498, 1977.
7. Whitney, Warren J.; et al.: Cold-Air Investigation of a 4½-Stage Turbine with Stage Loading Factor of 4.66 and High Specific Work Output. II—Stage Group Performance. NASA TP-1688, 1980.
8. Stewart, Warner L.; and Glassman, Arthur J.: Analysis of Fan-Turbine Efficiency Characteristics in Terms of Size and Stage Number. NASA TM X-1581, 1968.
9. Aerodynamic Design of Axial Flow Compressors. NASA SP-36 (revised), 1965.
10. Horlock, J. H.: Axial Flow Turbines. Butterworth (London), 1966.
11. Zweifel, O.: Spacing of Turbo-Machine Blading, Especially with Large Annular Deflection. Eng. Dig., vol. 3, no. 11, Nov. 1946, pp. 568-570.
12. Zweifel, O.: Spacing of Turbo-Machine Blading, Especially with Large Annular Deflection. Eng. Dig., vol. 3, no. 12, Dec. 1946, pp. 381-383.

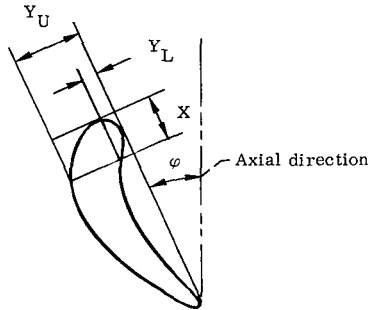
TABLE I. - PERTINENT BLADING DESIGN FEATURES

Blade row	Number of blades	Length, l , cm	Mean-radius chord, C_m , cm	Mean-radius chord spacing ratio, C_m/S_m	Aspect ratio, l/C_m	Mean-radius Zweifel coefficient	Leading-edge radius, cm	Trailing-edge radius, cm	Reaction at mean radius, ^a R_x
Stator 1	60	3.96	3.31	1.38	1.20	0.84	0.089	0.025	0.872
Rotor 1	78	4.57	2.87	1.56	1.59	.95	.051	.030	.442
Stator 2	86	5.52	2.84	1.70	1.94	.85	↓	.025	.387
Rotor 2	78	6.79	2.86	1.55	2.37	.94		.030	.430
Stator 3	89	8.19	2.84	1.76	2.88	.85		.025	.320
Rotor 3	81	9.65	2.85	1.61	3.38	.94		.030	.456
Stator 4	99	10.97	2.83	1.95	3.88	.85	↓	.025	.279
Rotor 4	83	12.7	2.87	1.66	4.42	.95		.030	.465
Outlet turning vanes	80	12.7	4.47	2.49	2.84	----	.013	.013	-.91

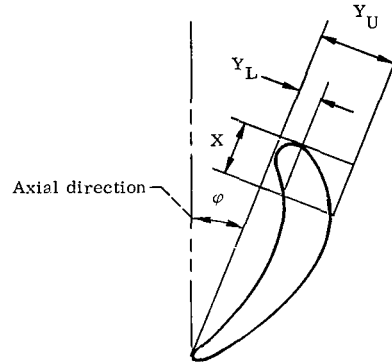
^a R_x reaction based on velocity change across blade row: $R_x = 1 - (V_2/V_1)^2$ for stator blade rows; $R_x = 1 - (W_2/W_1)^2$ for rotor blade rows.

TABLE II. - BLADE COORDINATES

(a) Stator blade



(b) Rotor blade



X, cm	Hub		Mean		Tip	
	Section radius, cm					
	20.879		22.860		24.841	
	Orientation angle, ϕ , deg					
	49.43		46.18		43.42	
	Y_L , cm	Y_U , cm	Y_L , cm	Y_U , cm	Y_L , cm	Y_U , cm
0	0.089	0.089	0.089	0.089	0.089	0.089
.127	.086	.279	.083	.305	.079	.295
.254	.086	.386	.083	.432	.079	.437
.381	.152	.454	.145	.518	.137	.541
.508	.205	.503	.196	.579	.185	.620
.635	.249	.533	.231	.617	.224	.671
.762	.274	.549	.262	.637	.257	.701
.889	.292	.554	.282	.648	.279	.719
1.016	.300	.546	.295	.645	.297	.724
1.143	.302	.536	.305	.635	.310	.719
1.270	.297	.518	.307	.617	.315	.706
1.397	.290	.498	.305	.594	.318	.688
1.524	.279	.472	.300	.569	.312	.665
1.651	.264	.447	.290	.544	.307	.640
1.778	.249	.422	.274	.513	.300	.610
1.905	.229	.391	.259	.483	.287	.579
2.032	.208	.361	.241	.452	.272	.549
2.159	.185	.330	.221	.419	.257	.516
2.286	.160	.295	.201	.384	.239	.480
2.413	.135	.259	.178	.348	.218	.444
2.540	.109	.221	.152	.310	.198	.409
2.667	.084	.180	.127	.269	.178	.368
2.794	.056	.140	.102	.229	.152	.328
2.921	.028	.099	.074	.188	.127	.284
3.048	-----	-----	.048	.142	.102	.239
3.076	.025	.025	-----	-----	-----	-----
3.175	-----	-----	.023	.094	.076	.193
3.302	-----	-----	-----	-----	.048	.147
3.312	-----	-----	.025	.025	-----	-----
3.429	-----	-----	-----	-----	.023	.097
3.564	-----	-----	-----	-----	.025	.025

X, cm	Hub		Mean		Tip	
	Section radius, cm					
	20.574		22.860		25.146	
	Orientation angle, ϕ , deg					
	8.48		13.30		14.48	
	Stacking axis coordinates, cm					
	X = 1.199	Y = 0.963	X = 1.184	X = 0.914	Y = 1.184	Y = 0.859
Y_L , cm	Y_U , cm	Y_L , cm	Y_U , cm	Y_L , cm	Y_U , cm	
0	0.038	0.038	0.051	0.051	0.063	0.063
.127	.117	.493	.081	.478	.040	.391
.254	.322	.765	.295	.754	.234	.635
.381	.498	.975	.480	.970	.401	.833
.508	.574	1.067	.627	1.146	.541	1.003
.635	.757	1.283	.747	1.278	.655	1.153
.762	.851	1.384	.833	1.361	.749	1.250
.889	.919	1.455	.899	1.415	.820	1.321
1.016	.970	1.501	.945	1.445	.873	1.361
1.143	1.001	1.521	.972	1.453	.909	1.379
1.270	1.013	1.519	.986	1.438	.930	1.377
1.397	1.016	1.494	.980	1.405	.935	1.354
1.524	1.001	1.450	.963	1.351	.925	1.311
1.651	.970	1.384	.927	1.278	.902	1.245
1.778	.927	1.300	.879	1.186	.861	1.163
1.905	.871	1.196	.815	1.085	.807	1.062
2.032	.790	1.077	.734	.975	.737	.955
2.159	.693	.945	.642	.859	.650	.841
2.286	.579	.803	.536	.737	.551	.721
2.413	.450	.648	.422	.602	.439	.594
2.540	.300	.480	.297	.460	.318	.460
2.667	.142	.297	.168	.307	.185	.315
2.794	-----	.094	.036	.147	.053	.162
2.824	.030	.030	-----	-----	-----	-----
2.870	-----	-----	.030	.030	-----	-----
2.888	-----	-----	-----	-----	.030	.030

1. Report No. NASA TP-1780	2. Government Accession No.	3. Recipient's Catalog No.
4. Title and Subtitle COLD-AIR INVESTIGATION OF FIRST STAGE OF $4\frac{1}{2}$ -STAGE, FAN-DRIVE TURBINE WITH AVERAGE STAGE-LOADING FACTOR OF 4.66	5. Report Date January 1981	6. Performing Organization Code
	8. Performing Organization Report No. E-461	10. Work Unit No. 505-32
7. Author(s) Warren J. Whitney, Thomas P. Moffitt, and Frank P. Behning	11. Contract or Grant No.	13. Type of Report and Period Covered Technical Paper
9. Performing Organization Name and Address National Aeronautics and Space Administration Lewis Research Center Cleveland, Ohio 44135	14. Sponsoring Agency Code	
	12. Sponsoring Agency Name and Address National Aeronautics and Space Administration Washington, D. C. 20546	
15. Supplementary Notes		
16. Abstract The design procedure and the development of the blading geometry for the $4\frac{1}{2}$ -stage turbine are discussed. The experimental results obtained with the first stage, operated as a single-stage turbine, are presented. The design procedure showed that a free-vortex design could meet the design requirements without incurring any serious problems such as excessive turning, negative reaction, or high Mach number. The results of the cold-air tests of the single-stage turbine showed that the turbine developed design work (stage-loading factor of 5.26) at an efficiency of 0.86, which was the efficiency predicted by a reference method. The mass flow at this condition was 1.024 of the design value. The highest efficiency obtained over the range of test conditions was 0.88, which occurred at design speed and a pressure ratio of 1.407, corresponding to a stage-loading factor of 4.35. The efficiency at this condition was 0.003 higher than that predicted by the reference method.		
17. Key Words (Suggested by Author(s)) Turbine aerodynamics High stage loading	18. Distribution Statement Unclassified - unlimited	Subject Category 07
19. Security Classif. (of this report) Unclassified	20. Security Classif. (of this page) Unclassified	21. No. of Pages 14
		22. Price* A02

* For sale by the National Technical Information Service, Springfield, Virginia 22161

National Aeronautics and
Space Administration

Washington, D.C.
20546

Official Business

Penalty for Private Use, \$300

SPECIAL FOURTH CLASS MAIL
BOOK

Postage and Fees Paid
National Aeronautics and
Space Administration
NASA-451



11 1 1U,A, 121980 S00903DS
DEPT OF THE AIR FORCE
AF WEAPONS LABORATORY
ATTN: TECHNICAL LIBRARY (SUL)
KIRTLAND AFB NM 87117

NASA

POSTMASTER: If Undeliverable (Section 158
Postal Manual) Do Not Return
